Responses of land evapotranspiration to Earth's greening in CMIP5 Earth System Models

2016 Environ. Res. Lett. 11 104006

(http://iopscience.iop.org/1748-9326/11/10/104006)

Environmental Research Letters

LETTER

Responses of land evapotranspiration to Earth's greening in CMIP5 Earth System Models

Zhenzhong Zeng[1], **Zaichun Zhu**[1], **Xu Lian**[1], **Laurent Z X Li**[2], **Anping Chen**[3], **Xiaogang He**[4] **and Shilong Piao**[1,5]

[1] Sino-French Institute for Earth System Science, College of Urban and Environmental Sciences, Peking University, Beijing 100871, People's Republic of China
[2] Laboratoire de Météorologie Dynamique, Centre National de la Recherche Scientifique, Université Pierre et Marie Curie-Paris 6, F-75252 Paris, France
[3] The Woods Hole Research Center, Falmouth, MA 02540, USA
[4] Department of Civil and Environmental Engineering, Princeton University, NJ 08544, USA
[5] Institute of Tibetan Plateau Research, Chinese Academy of Sciences, Beijing 100085, People's Republic of China

E-mail: slpiao@pku.edu.cn

Keywords: evapotranspiration sensitivity to greening, Earth greening, leaf area index, land–climate interaction, Earth System Modelling

Supplementary material for this article is available online

OPEN ACCESS

RECEIVED
16 May 2016

REVISED
4 September 2016

ACCEPTED FOR PUBLICATION
16 September 2016

PUBLISHED
3 October 2016

Abstract

Satellite-observed Earth's greening has been reproduced by the latest generation of Earth System Models (ESMs) participating in the Coupled Model Intercomparison Project Phase 5 (CMIP5). Land evapotranspiration (ET) is expected to rise with increasing leaf area index (LAI, Earth's greening). The responses of ET play a key role in the land–climate interaction, but they have not been evaluated previously. Here, we assessed the responses of ET to Earth's greening in these CMIP5 ESMs. We verified a significant and positive response of ET to the modeled greening in each model. However, the responses were not comparable across the ESMs because of an inherent bias in the sensitivity of ET to LAI ($\partial ET/\partial LAI$) in the models: $\partial ET/\partial LAI$ is precisely and inversely proportional to the trend of LAI ($\partial LAI/\partial t$) across the ESMs. Constrained by this inversely proportional relationship with the satellite-observed $\partial LAI/\partial t$, the Earth's $\partial ET/\partial LAI$ is 0.26 (0.21–0.34) mm d^{-1} per m^2 m^{-2}, equaling the independent estimates from satellite-derived reconstructions of ET and LAI. Thus, the Earth's greening-induced acceleration of ET is about 11.4 mm yr^{-1}, accounting for more than 50% of the observed increase in land ET over the last 30 years. To better model the land–climate interaction, $\partial ET/\partial LAI$ in these ESMs should be calibrated. A feasible means is to improve the representation of the magnitude of LAI in these CMIP5 ESMs.

1. Introduction

The greening of the Earth over the last three decades has been documented by several studies based on the National Oceanic and Atmospheric Administration-Advanced Very High Resolution Radiometer (NOAA-AVHRR) satellite records (e.g., Nemani *et al* 2003, Zhu *et al* 2013, 2016, Dardel *et al* 2014, Piao *et al* 2015), matching the long-term forest inventories (McMahon *et al* 2010, Fang *et al* 2014) and enhanced seasonal exchange of CO_2 (Graven *et al* 2013, Forkel *et al* 2016). The Earth's greening, defined as an increase in leaf area index (LAI) over land, seems to have been reproduced by most state-of-the-art Earth System Models (ESMs) participating in the Coupled Model Intercomparison Project Phase 5 (CMIP5) (Taylor *et al* 2012, Mahowald *et al* 2015). Furthermore, these ESMs also unequivocally and consistently project continuation of Earth's greening, at least until the end of the 21st century (Mahowald *et al* 2015). As the change in land surface properties has a profound impact on land–atmosphere exchanges of water and energy, and ultimately on the climate system, the modeled Earth's greening should incorporate boundary forcing in these climate model simulations.

The key flux determining the strength of the greening-induced boundary forcing is terrestrial evapotranspiration (ET). ET, as a central process in the climate system, represents the exchanges of energy and water between the land and the atmosphere. As for its

driver, because transpiration through vegetation crown dominates terrestrial ET (Jasechko *et al* 2013), the greening of the Earth has been one of the most important drivers in the rise of global land ET over the past 30 years (Zhang *et al* 2015). As for its effect, terrestrial ET plays a fundamental role in shaping the climate. It cools the land surface temperature by consuming more than half of the solar radiation absorbed by the land surface (Trenberth *et al* 2009), and drives atmospheric dynamics by the released latent heat during condensation (Makarieva *et al* 2013). Therefore, the greening of the Earth would be expected to reshape the Earth's climate (e.g., rainfall, temperature, and circulation) by producing evapotranspiration (Shukla and Mintz 1982, Bounoua *et al* 2000, Sewall *et al* 2000, Buermann *et al* 2001).

In the ESMs, the response of ET to the modeled Earth's greening determines the strength of vegetation feedback in the land–climate interaction. Assuming that all CMIP5 ESMs simulated the sensitivity of ET to LAI (∂ET/∂LAI) following the laws of nature, ∂ET/∂LAI in these ESMs should be close to the Earth's ∂ET/∂LAI, resulting in a tendency to be constant across the models. Terrestrial ET increased more in the ESMs with a higher greening rate (∂LAI/∂t); thus a stronger evaporative cooling effect and faster moisture recycling were modeled. That is, greening-induced boundary forcing was underestimated (or overestimated) by ESMs that modeled a weaker (or stronger) greening rate than the satellite-observed greening rate. This implies that, to better model the land–climate interaction in the ESMs, the modeling community should focus on improving the simulation of vegetation dynamics (i.e., ∂LAI/∂t).

To our knowledge, however, no evaluation of the responses of ET to the Earth's greening in these CMIP5 ESMs has been performed. If biases exist in the modeled ∂ET/∂LAI, the greening-induced boundary forcing would not be comparable across the ESMs. In this case, it is important to understand why the modeled ∂ET/∂LAI differs from the ESMs. In addition, the modeling community should pay more attention to calibration of the representation of the sensitivity of ET to greening (i.e., ∂ET/∂LAI).

In this study, we assessed the responses of ET to Earth's greening in the CMIP5 ESMs by integrating the historical simulations from CMIP5 ESMs with satellite-derived reconstructions of ET and LAI over the last 30 years. The objective was to address the following questions (1) is there a significant and positive response of land ET to Earth's greening in each ESM? A positive answer to this question would verify that land LAI is an important driver of the interannual variation of land ET in the ESMs. (2) Is ∂ET/∂LAI constant across the ESMs? If the answer is positive, we would expect a greater increase in land ET in the ESMs with a higher greening rate. A negative answer would prompt us to ask, (3) why does the modeled ∂ET/∂LAI differ among the CMIP5 ESMs, how great is the Earth's ∂ET/∂LAI, and how can we calibrate the modeled ∂ET/∂LAI to better model the land–climate interaction?

2. Methods and datasets

2.1. Model datasets

We made use of the historical simulations by the latest generation of ESMs that participated in CMIP5 (Taylor *et al* 2012, Stocker *et al* 2013). A summary of the CMIP5 ESMs used in this study is provided in table 1. A total of 27 ESMs from 14 modeling centers were chosen based on their data availability. The outputs of both LAI (in $m^2\ m^{-2}$) and ET (in mm d^{-1}) in the historical simulations of these ESMs were downloaded from the CMIP5 archive (http://pcmdi9.llnl.gov/). The annual area-weighted global land-average LAI and ET during 1982–2005 were calculated using the average of all initial condition ensemble members available in the archive.

2.2. Observational datasets

The long-term NOAA-AVHRR satellite measurements were used to generate an 8 km global LAI product from 1982 to 2011 (AVHRR GIMMS LAI3g) (Zhu *et al* 2013). The quality of the satellite LAI product used in this study has been extensively evaluated through the comparisons with field measurements, with an accuracy of about 0.68 $m^2\ m^{-2}$ (root mean square error) relative to field measured LAI (Zhu *et al* 2013). This product has been validated as a research-quality dataset (e.g., Zhu *et al* 2013, Pfeifer *et al* 2014) and has been extensively used in the research of long-term vegetation dynamics (e.g., Zhu *et al* 2013, 2016, Anav *et al* 2013a, Dardel *et al* 2014, Piao *et al* 2015, Sitch *et al* 2015).The annual area-weighted global land-average LAI during 1982–2011 was calculated from this dataset.

No direct observations of global land ET over the last 30 years have been reported. In this study, we included five satellite-derived reconstructions of long-term evapotranspiration over land: FLUXNET-MTE ET (1982–2008, based on eddy-covariance measurements Jung *et al* 2010), GRACE-MTE ET (1982–2011, based on water mass balance Zeng *et al* 2014), and three offline evapotranspiration algorithm-based products, MPM ET (Zhang *et al* 2010), P-LSH ET (Zhang *et al* 2015), and PML ET (Zhang *et al* 2016) (details see table 2). All these products have been proven of quality for scientific researches. Yet, because of the lack of direct global observations, it is hard to estimate the biases in these products and to tell which product is superior to the others. Thus, all these products were applied to calculate the annual area-weighted global land-average ET of the last three decades, with the difference among them representing an uncertainty range in the observed land ET. The Earth's sensitivity

Table 1. Summary of the CMIP5 Earth System Models analyzed in this study.

Model name	Modeling center	Institute
ACCESS1-0	CSIRO-BOM	CSIRO (Commonwealth Scientific and Industrial Research Organisation, Australia), and BOM (Bureau of Meteorology, Australia)
ACCESS1-3		
BNU-ESM	GCESS	College of Global Change and Earth System Science, Beijing Normal University
CCSM4	NCAR	National Center for Atmospheric Research
CESM1-BGC	NSF-DOE-NCAR	National Science Foundation, Department of Energy, National Center for Atmospheric Research
CESM1-CAM5		
CESM1-WACCM		
CanESM2	CCCma	Canadian Centre for Climate Modelling and Analysis
FIO-ESM	FIO	The First Institute of Oceanography, SOA, China
GFDL-CM3	NOAA GFDL	Geophysical Fluid Dynamics Laboratory
GFDL-ESM2G		
GFDL-ESM2M		
HadGEM2-CC	MOHC	Met Office Hadley Centre (additional HadGEM2-ES realizations contributed by Instituto Nacional de Pesquisas Espaciais)
HadGEM2-ES		
IPSL-CM5A-LR	IPSL	Institut Pierre-Simon Laplace
IPSL-CM5A-MR		
IPSL-CM5B-LR		
MIROC-ESM	MIROC	Atmosphere and Ocean Research Institute (The University of Tokyo), National Institute for Environmental Studies, and Japan Agency for Marine-Earth Science and Technology
MIROC-ESM-CHEM		
MIROC5		
MPI-ESM-LR	MPI-M	Max Planck Institute for Meteorology (MPI-M)
MPI-ESM-MR		
NorESM1-M	NCC	Norwegian Climate Centre
NorESM1-ME		
bcc-csm1-1	BCC	Beijing Climate Center, China Meteorological Administration
bcc-csm1-1-m		
inmcm4	INM	Institute for Numerical Mathematics

of ET to LAI (∂ET/∂LAI) was thus estimated with these observed land ET and LAI over the last 30 years.

3. Results and discussion

3.1. Response of land ET to Earth's greening in each CMIP5 ESM

The magnitude of land LAI found among the CMIP5 ESMs covered a large spectrum, and most models overestimated the magnitude of land LAI compared to observations from the AVHRR satellites (figure 1(a)), probably due to the systematic underestimate of NPP in these models (Shao *et al* 2013, Anav *et al* 2013b). Despite this, the greening of the Earth, defined as a significant and positive trend of land LAI observed from the AVHRR satellites for the last 30 years (e.g., Zhu *et al* 2013, 2016, Piao *et al* 2015), was reproduced by 16/27 CMIP5 ESMs (figure 1(b)). For the other 11/27 ESMs, land LAI either did not vary annually (ACCESS1-0, ACCESS1-3, FIO-ESM), decreased unreasonably by a constant rate each year (MIROC5, figure S1), or did not change significantly over the last 30 years (CESM1-WACCM, CanESM2, GFDL-ESM2M, MIROC-ESM, MPI-ESM-LR, NorESM1-ME, inmcm4). Land LAI, if not fixed in models, is a key driving factor of interannual variation of land ET in all the models (figures 1(c) and S2). As the goal of this study is to investigate the responses of land ET to Earth's greening in CMIP5 ESMs, we analyzed the responses of land ET to increasing LAI in the 16 CMIP5 ESMs that successfully reproduced the Earth's greening of the last 30 years (figure 1(c)).

As shown in figure 1(c), there was a significant interannual correlation between the modeled land LAI and ET for all 16 ESMs that reproduced the Earth's greening. The strongest correlation between the modeled land LAI and ET was found in GFDL-CM3 (figure 1(c5), $R = 0.81$, $P < 0.01$), and the weakest correlation was found in CESM1-CAM5 (figure 1(c4), $R = 0.35$, $P < 0.1$). Consistent with the significant correlation, land ET increased significantly with

Table 2. Descriptions of the five long-term global land ET products used in this study.

product	reference	period	algorithm	drivers
FLUXNET-MTE	Jung *et al* (2010)	1982–2008	Combined with FLUXNET and the model tree ensemble	Climate: precipitation, temperature Vegetation: fAPAR
GRACE-MTE	Zeng *et al* (2014)	1982–2011	Combined with water balance and the model tree ensemble	Climate: precipitation, temperature, radiation, pressure, vapor pressure, wind speed, wet day frequency, frost day frequency Vegetation: NDVI
MPM	Zhang *et al* (2010)	1983–2006	Modified Penman–Monteith approach	Climate: radiation, temperature, air water vapor pressure Vegetation: NDVI
P-LSH	Zhang *et al* (2015)	1982–2013	Process-based Land Surface Evapotranspiration Heat Fluxes algorithm	Climate: radiation, temperature, air water vapor pressure, wind speed, vegetation, CO_2 Vegetation: NDVI
PML	Zhang *et al* (2016)	1981–2012	Penman–Monteith–Leuning model	Climate: precipitation, air temperature, vapor pressure, shortwave downward radiation, longwave downward radiation and wind speed Vegetation: LAI, emissivity and albedo

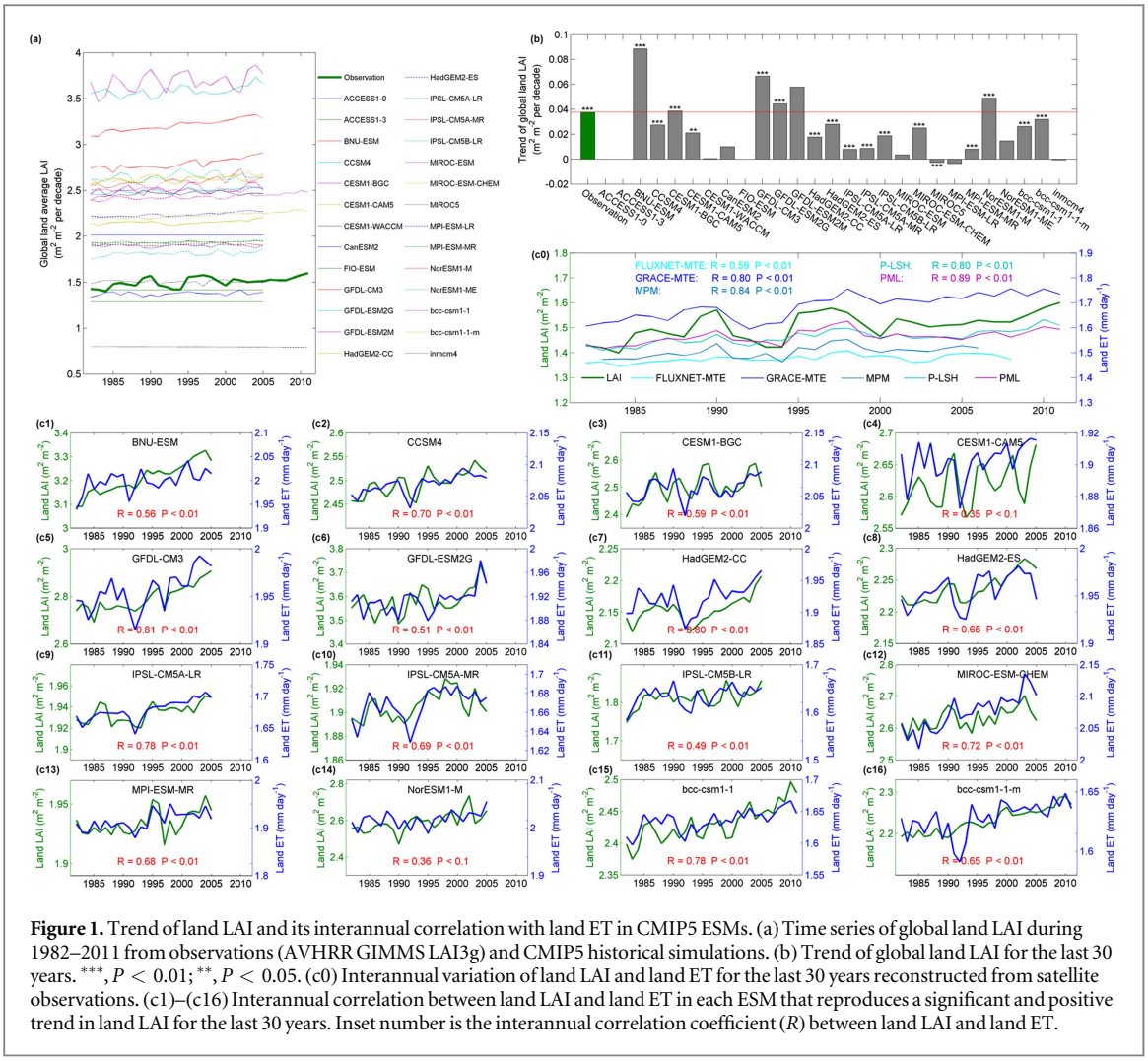

Figure 1. Trend of land LAI and its interannual correlation with land ET in CMIP5 ESMs. (a) Time series of global land LAI during 1982–2011 from observations (AVHRR GIMMS LAI3g) and CMIP5 historical simulations. (b) Trend of global land LAI for the last 30 years. ***, $P < 0.01$; **, $P < 0.05$. (c0) Interannual variation of land LAI and land ET for the last 30 years reconstructed from satellite observations. (c1)–(c16) Interannual correlation between land LAI and land ET in each ESM that reproduces a significant and positive trend in land LAI for the last 30 years. Inset number is the interannual correlation coefficient (R) between land LAI and land ET.

increasing LAI in all 16 ESMs (figure 1(c)). That is, land ET responded positively to the modeled Earth's greening in all of the models. Land LAI indeed is a key driver of the interannual variability in land ET in each ESM (e.g., Zhang *et al* 2015).

In theory, LAI is one of the key parameters of land ET which is also co-determined by factors like soil moisture supply, solar radiation, and wind speed. LAI could change land ET by its role in the regulations of the surface area of vegetation in direct contact with the atmosphere and thus the efficiency by which water can be transferred from within the vegetation to the atmosphere (e.g., canopy conductance g_c), surface radiation budget (e.g., albedo, and radiation partitioning between canopy and soil), boundary layer aerodynamic characteristics (e.g., aerodynamic conductance), and redistribution of rainfall (e.g., interception and through fall). Among them, regulating the canopy conductance (g_c) has been suggested as a dominant one by dozens of studies (e.g., Sellers *et al* 1997, Zeng *et al* 1999, Bonan 2002, Krinner *et al* 2005, Kala *et al* 2013, Zhang *et al* 2015). The regulation of LAI on the canopy conductance (g_c) is often formatted as $g_c = g_{smax}\beta(w)f(\mathrm{LAI})$, where g_{smax} is the leaf-level maximum conductance, and $\beta(w)$ is a soil moisture stress scalar. Based on the results of field experiments, the theoretical function f (LAI) is widely described in land surface models (e.g., Zeng *et al* 1999, Krinner *et al* 2005, Oleson *et al* 2010) as

$$f(\mathrm{LAI}) = \frac{1}{i_1\dfrac{1}{\mathrm{LAI}} + i_2} \quad (1)$$

or

$$f(\mathrm{LAI}) = (1 - e^{-j\cdot\mathrm{LAI}})/j, \quad (2)$$

where i_1, i_2, and j are parameters that are dependent on aerodynamic roughness and vegetation type. Figure 2 shows the curves of equations (1) and (2) with $i_1 = 1$, $i_2 = 1$, and $j = 1$, which clearly demonstrates that, in each ESM, land ET should increase with LAI.

3.2. Responses of land ET to Earth's greening across CMIP5 ESMs

As 1) land ET responds to the modeled greening in each ESM (figures 1(c)) and 2) the greening rate (i.e., $\partial\mathrm{LAI}/\partial t$) differs among the models (figure 1(b)), the increase in land ET ($\partial\mathrm{ET}/\partial t$) is expected to be greater in the ESMs with a higher greening rate, i.e., $\dfrac{\partial \mathrm{ET}}{\partial t} \propto \dfrac{\partial \mathrm{LAI}}{\partial t}$. However, as shown in figure 3, there is no correlation between the modeled $\partial\mathrm{ET}/\partial t$ and

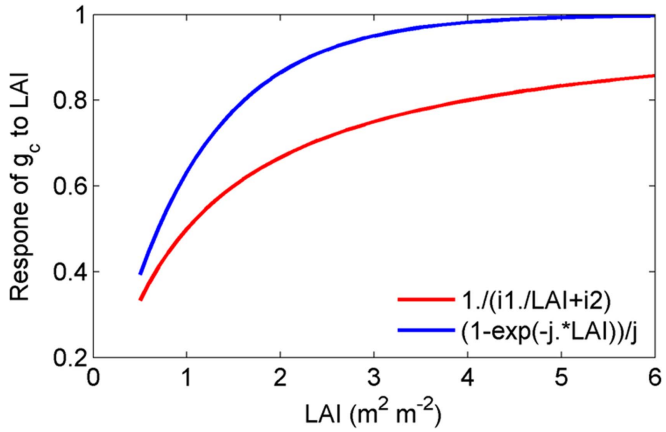

Figure 2. Examples of the negative exponential curve used to represent canopy conductance, g_c, as a function of LAI for parameters $i_1 = 1$, $i_2 = 1$, $j = 1$ in equations (1) and (2).

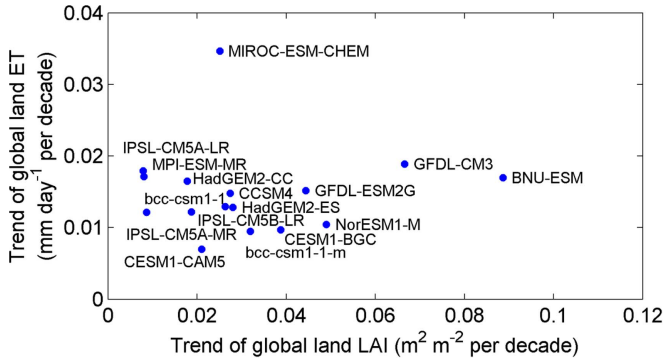

Figure 3. Trend of global land ET versus trend of global land LAI across the CMIP5 ESMs.

$\partial\mathrm{LAI}/\partial t$ across the ESMs ($R = 0.03$, $P = 0.90$). Although $\partial\mathrm{LAI}/\partial t$ differs among the models, $\partial\mathrm{ET}/\partial t$ remains constant (~0.01 mm d^{-1} per decade) across models (figure 3), indicating that the sensitivity of land ET to land LAI ($\partial\mathrm{ET}/\partial\mathrm{LAI}$) varies across the ESMs.

Indeed, we found an inherent bias in the modeled $\partial\mathrm{ET}/\partial\mathrm{LAI}$ that causes the lack of correlation between $\partial\mathrm{LAI}/\partial t$ and $\partial\mathrm{ET}/\partial t$ across the ESMs (figure 4). $\partial\mathrm{ET}/\partial\mathrm{LAI}$ is significantly and inversely proportional to $\partial\mathrm{LAI}/\partial t$ across the CMIP5 ESMs. That is, $\dfrac{\partial\mathrm{ET}}{\partial\mathrm{LAI}} = 0.01 \Big/ \dfrac{\partial\mathrm{LAI}}{\partial t}$ ($R = 0.91$, $P < 0.01$; figure 4). Given that $\dfrac{\partial\mathrm{ET}}{\partial t} = \dfrac{\partial\mathrm{ET}}{\partial\mathrm{LAI}} \cdot \dfrac{\partial\mathrm{LAI}}{\partial t} = \left(0.01 \Big/ \dfrac{\partial\mathrm{LAI}}{\partial t}\right) \cdot \dfrac{\partial\mathrm{LAI}}{\partial t} = 0.01$ mm d^{-1} per decade, $\partial\mathrm{ET}/\partial t$ across the ESMs tends to be constant, as shown in figure 3. This explains the lack of correlation between $\partial\mathrm{ET}/\partial\mathrm{LAI}$ and $\partial\mathrm{LAI}/\partial t$ across the ESMs (figure 3).

We then investigated why $\partial\mathrm{ET}/\partial\mathrm{LAI}$ is inversely proportional to $\partial\mathrm{LAI}/\partial t$ across the ESMs. In theory, as shown in figure 2, while ET increases with LAI in each ESM, $\partial\mathrm{ET}/\partial\mathrm{LAI}$ decreases with the magnitude of LAI across the ESMs, which is also shown in the partial derivatives to LAI for equations (1) and (2):

$$\frac{\partial\mathrm{ET}}{\partial\mathrm{LAI}} \propto \frac{\partial f(\mathrm{LAI})}{\partial\mathrm{LAI}} = \frac{i_1}{(i_1 + i_2\mathrm{LAI})^2} \tag{3}$$

and

$$\frac{\partial\mathrm{ET}}{\partial\mathrm{LAI}} \propto \frac{\partial f(\mathrm{LAI})}{\partial\mathrm{LAI}} = \mathrm{e}^{-\mathrm{j}\cdot\mathrm{LAI}}. \tag{4}$$

Thus, the inherent bias of $\partial\mathrm{ET}/\partial\mathrm{LAI}$ is primarily due to the bias in the magnitude of LAI across the CIMP5 ESMs (figure 1(a)). In addition, the bias in the magnitude of LAI is also responsible for the difference in $\partial\mathrm{LAI}/\partial t$ across the models: $\partial\mathrm{LAI}/\partial t$ is significantly proportional to the magnitude of land LAI across the models ($P < 0.01$; figure 5). As a result, $\partial\mathrm{ET}/\partial\mathrm{LAI}$ is inversely proportional to $\partial\mathrm{LAI}/\partial t$ across the CMIP5 ESMs (figure 4).

3.3. The Earth's sensitivity of land ET to land LAI

If all the ESMs modeled the land–climate interaction well, the modeled sensitivity of land ET to land LAI should be almost constant across the models, with the constant being the Earth's $\partial\mathrm{ET}/\partial\mathrm{LAI}$. However, due to the bias in the magnitude of modeled LAI (figure 1(a)), there are biases in the modeled $\partial\mathrm{ET}/\partial\mathrm{LAI}$ in the CMIP5 ESMs. To better model the land–climate interaction, $\partial\mathrm{ET}/\partial\mathrm{LAI}$ in these ESMs should be calibrated to equal the Earth's $\partial\mathrm{ET}/\partial\mathrm{LAI}$.

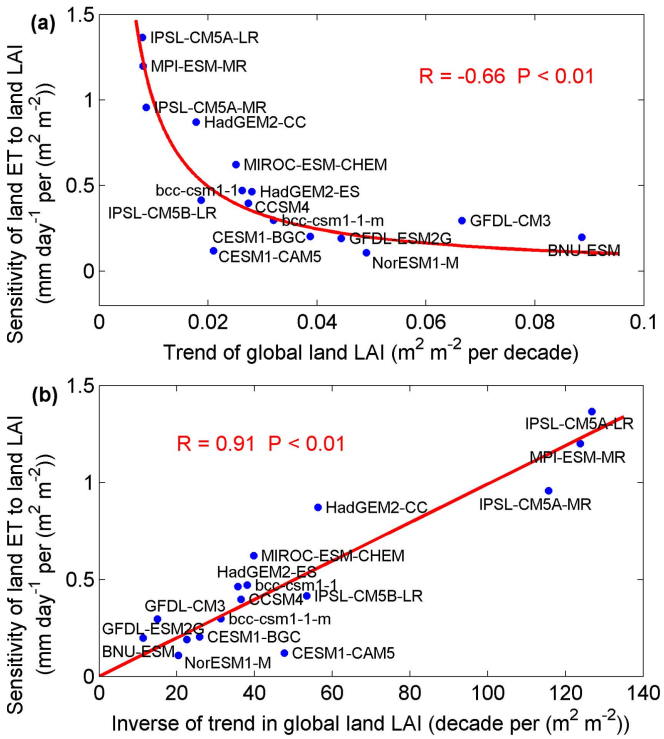

Figure 4. Sensitivity of land ET to land LAI versus (a) trend in global land LAI, and versus (b) inverse of trend in global land LAI across the CMIP5 ESMs.

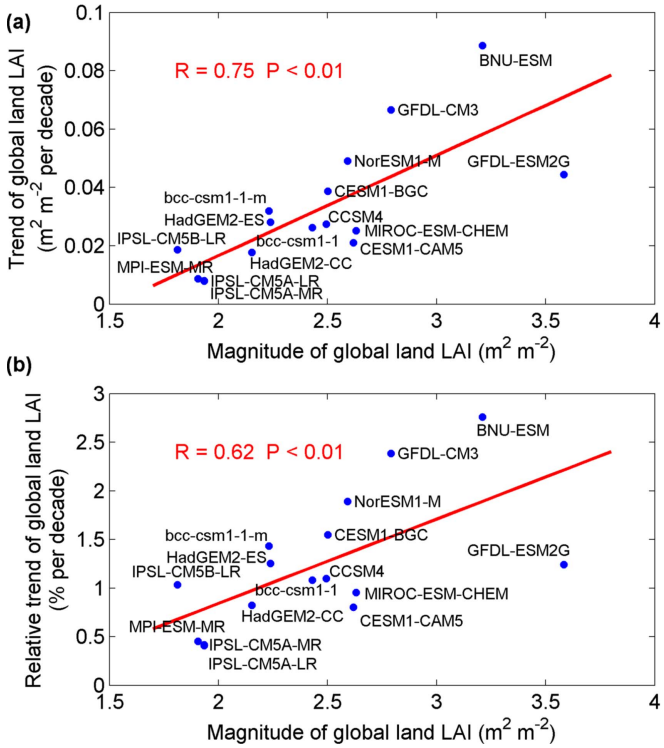

Figure 5. Trend of global land LAI versus magnitude of global land LAI across the CMIP5 ESMs. (a) Absolute trend of land LAI, and (b) relative trend of land LAI.

Here, we further applied two approaches to provide a reference for the Earth's $\partial ET/\partial LAI$ making use of model simulations from CMIP5 and satellite observations of ET and LAI over the last 30 years.

First, the Earth's $\partial ET/\partial LAI$ can be estimated by the observational constraints on the precise inversely proportional relationship between the modeled $\partial ET/\partial LAI$ and $\partial LAI/\partial t$ across the CMIP5 ESMs. As

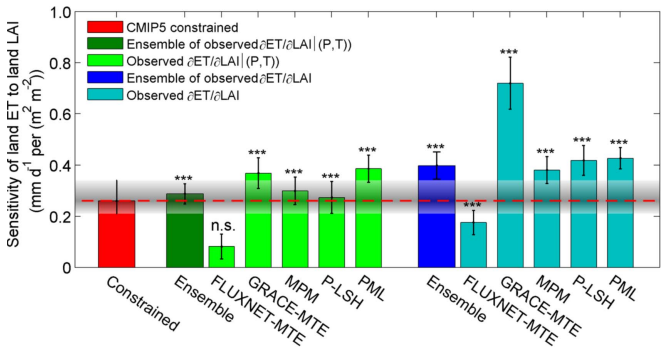

Figure 6. The Earth's sensitivity of land ET to land LAI estimated from the observational constraint on the CMIP5 ESMs (red bar), and the linear regressions of satellite-derived reconstructions of ET and LAI over the last 30 years (blue and green bars). For the sensitivity from the observational constraint, the error bar shows the range constrained by the mean ± standard error (SE) of the satellite-observed trend in global land LAI. For the sensitivities of the regressions, ***, $P < 0.01$; n.s., $P > 0.05$ for sensitivity, and error bars show the standard errors of the sensitivities.

shown in figure 4, the modeled $\partial ET/\partial LAI$ ranges from 0.11 to 1.37 mm d^{-1} per m^2 m^{-2} in the ESMs, and the inversely proportional relationship across the ESMs is $\frac{\partial ET}{\partial LAI} = 0.01 \Big/ \frac{\partial LAI}{\partial t}$ ($R = 0.91$, $P < 0.01$; figure 4). The satellite-observed trend of land LAI over the last 30 years, i.e., $\partial LAI/\partial t$, is 0.04 ± 0.01 m^2 m^{-2} per decade (figure 1(b)) (Zhu *et al* 2013). We constrained the modeled inversely proportional relationship with the observed $\partial LAI/\partial t$, and estimated the Earth's $\partial ET/\partial LAI$ to be 0.26 (0.21–0.34) mm d^{-1} per m^2 m^{-2} (red bar in figure 6).

Second, we applied the satellite-derived reconstructions of ET and LAI during the last 30 years to provide an independent estimate of the Earth's $\partial ET/\partial LAI$. The annual area-weighted global land-average ET and LAI for the last 30 years were substituted into the linear regression equation, $ET = k_1 LAI + c_1$, where k_1 is the sensitivity. The observed $\partial ET/\partial LAI$ is 0.18 ± 0.05 mm d^{-1} per m^2 m^{-2} using FLUXNET-MTE ET (Jung *et al* 2010), 0.72 ± 0.10 mm d^{-1} per m^2 m^{-2} using GRACE-MTE ET (Zeng *et al* 2014), 0.38 ± 0.05 mm d^{-1} per m^2 m^{-2} using MPM ET (Zhang *et al* 2010), 0.42 ± 0.06 mm d^{-1} per m^2 m^{-2} using P-LSH ET (Zhang *et al* 2015), and 0.43 ± 0.04 mm d^{-1} per m^2 m^{-2} using PML ET (Zhang *et al* 2016) (light blue bars in figure 6). As the observed LAI and ET could vary with other factors simultaneously, we further calculated the observed $\partial ET/\partial LAI$ with the linear regression equation controlling precipitation and temperature, i.e., $ET = k_2 LAI + c_2 P + c_3 T + c_4$, where P and T are the observed annual precipitation and annual average temperature from the CRU dataset, respectively (Harris *et al* 2014), and k_2 is the sensitivity controlling precipitation and temperature. In this approach, the observed $\partial ET/\partial LAI$ ranges from 0.08 to 0.39 mm d^{-1} per m^2 m^{-2} depending on ET products (green bars in figure 6). The ensemble of the observed $\partial ET/\partial LAI$ controlling precipitation and temperature provides the optimal estimate of the Earth's $\partial ET/\partial LAI$, namely 0.29 (0.25–0.33) mm d^{-1} per m^2 m^{-2} (dark green bar in figure 6).

Thus, the two independent estimates of the Earth's $\partial LAI/\partial t$ match very well with each other. Using the sensitivity estimated by the observational constraints, the satellite-observed Earth's greening (i.e., the increasing LAI at a rate of 0.04 ± 0.01 m^2 m^{-2} per decade) has accelerated land ET by 11.4 mm yr^{-1} in the past 30 years. The total increase in land ET during the last 30 years is 16.3 ± 6.9 mm yr^{-1} according to the CMIP5 ESMs, and ranges from 13.1 to 51.2 mm yr^{-1} according to the satellite-derived reconstructions of ET (average: 26.6 mm yr^{-1}), depending on the model and/or ET dataset used as a reference. Therefore, the Earth's greening-induced acceleration of ET has contributed more than 50% of the observed increase in land ET over the last 30 years. The greater capacity of water loss associated with increasing LAI has become a dominant driver of the increasing land ET in the past 30 years.

3.4. Implications for model improvement

Considering the key role of ET in the water cycle and energy fluxes, the biophysical feedback of vegetation growth activity should play an important role in shaping the climate. However, in the CMIP5 ESMs, the biophysical feedback of vegetation growth activity has not been represented well due to the biases in the greening rate ($\partial LAI/\partial t$) and the sensitivity of ET to greening ($\partial ET/\partial LAI$). The modeling community should calibrate the modeled $\partial ET/\partial LAI$ to make it equivalent to the Earth's $\partial ET/\partial LAI$ (~0.26 mm d^{-1} per m^2 m^{-2}). As the biases of both $\partial LAI/\partial t$ and $\partial ET/\partial LAI$ are primarily caused by the modeled bias of the magnitude of land LAI, feasible and effective methods for improving the representation of vegetation–climate feedback are therefore required to improve the representation of the magnitude of LAI in these state-of-the-art ESMs.

In addition, we found that magnitude of global land LAI of four ESMs was similar to the value observed by satellite (MPI-ESM-MR, IPSL-CM5B-LR,

IPSL-CM5A-LR, IPSL-CM5A-MR, see figure 5; the observed magnitude is 1.5 $m^2 m^{-2}$). However, all of these models still underestimated the trend in global land LAI compared to the satellite-observed trend (i.e., 0.04 $\pm$ 0.01 $m^2 m^{-2}$ per decade). Among these four models, the closer the modeled $\partial LAI/\partial t$ is to the satellite-observed trend, the closer the modeled $\partial ET/\partial LAI$ is to the Earth's $\partial ET/\partial LAI$ (figure 4(a)). Therefore, another work at a next stage for the modeling community is to investigate the mechanisms driving the temporal changes in land LAI (e.g., Piao *et al* 2015, Zhu *et al* 2016) and then improve the representation of temporal variation of LAI in the ESMs.

4. Conclusions

Our results demonstrated a significant and positive response of land ET to increasing LAI in all of the 16 CMIP5 ESMs that reproduced the Earth's greening for the last three decades. However, the responses of land ET to the modeled greening are not comparable across the ESMs due to an inherent bias in the modeled $\partial ET/\partial LAI$: $\partial ET/\partial LAI$ is precisely and inversely proportional to $\partial LAI/\partial t$ across the ESMs. Furthermore, this inherent bias in the modeled sensitivity was found to be primarily due to the bias in the magnitude of LAI. The bias in the modeled $\partial ET/\partial LAI$ indicates that greening-induced biophysical feedback has not been represented well in these ESMs. Thus, it is necessary to improve the representation of the magnitude of LAI, which is an easy, feasible, and effective means for an ESM to calibrate the response of land ET to greening and thus to better represent the climate effect of Earth's greening in the model.

We estimated the Earth's $\partial ET/\partial LAI$ with two independent approaches, including the observational constraints on the precise inversely proportional relationship between the modeled $\partial ET/\partial LAI$ and $\partial LAI/\partial t$ across the CMIP5 ESMs, and linear regression of the satellite-derived reconstructions of ET and LAI during the last 30 years. The suggested sensitivity of land ET to land LAI in the Earth's climate is ~0.26 mm d^{-1} per $m^2 m^{-2}$. With this sensitivity, the satellite-observed Earth's greening can be translated into acceleration of land ET by a rate of 3.8 mm yr^{-1} per decade, accounting for more than 50% of the observed acceleration rate of land ET over the last 30 years. As the response of land ET deeply affects the climate (water cycle and energy fluxes), it will be important to investigate the climate effect of Earth's greening by combining satellite-derived observations and the state-of-the-art ESMs. Furthermore, because the biophysical feedback induced by the response of land ET is dominated over the regions where vegetation has changed, the understanding of the climate effect of Earth's greening would improve future projections of regional climate change and benefit local policy decisions.

Acknowledgments

We are grateful to the World Climate Research Programme Working Group on Coupled Modelling and the climate modeling groups listed in table 1 for the model outputs of CMIP5. This study was supported by National Natural Science Foundation of China (41530528), and the 111 Project (B14001).

References

Anav A *et al* 2013a Evaluation of land surface models in reproducing satellite derived leaf area index over the high-latitude Northern Hemisphere: II. Earth system models *Remote Sens.* **5** 3637

Anav A *et al* 2013b Evaluating the land and ocean components of the global carbon cycle in the CMIP5 Earth System Models *J. Clim.* **26** 6801–43

Bonan G B 2002 *Ecological Climatology: Concepts and Applications* (Cambridge: Cambridge University Press)

Bounoua L *et al* 2000 Sensitivity of climate to changes in NDVI *J. Clim.* **13** 2277–92

Buermann W, Dong J, Zeng X, Myneni R B and Dickinson R E 2001 Evaluation of the utility of satellite-based vegetation leaf area index data for climate simulations *J. Clim.* **14** 3536–50

Dardel C, Kergoat L, Hiernaux P, Mougin E, Grippa M and Tucker C J 2014 Re-greening Sahel: 30 years of remote sensing data and field observations (Mali, Niger) *Remote Sens. Environ.* **140** 350–64

Fang J *et al* 2014 Evidence for environmentally enhanced forest growth *Proc. Natl Acad. Sci. USA* **111** 9527–32

Forkel M *et al* 2016 Enhanced seasonal CO_2 exchange caused by amplified plant productivity in northern ecosystems *Science* **351** 696–9

Graven H D *et al* 2013 Enhanced seasonal exchange of CO_2 by Northern ecosystems since 1960 *Science* **341** 1085–9

Harris I, Jones P D, Osborn T J and Lister D H 2014 Updated high-resolution grids of monthly climatic observations—the CRU TS3.10 dataset *Int. J. Climatol.* **34** 623–42

Jasechko S, Sharp Z D, Gibson J J, Birks S J, Yi Y and Fawcett P J 2013 Terrestrial water fluxes dominated by transpiration *Nature* **496** 347–50

Jung M *et al* 2010 Recent decline in the global land evapotranspiration trend due to limited moisture supply *Nature* **467** 951–4

Kala J *et al* 2013 Influence of leaf area index prescriptions on simulations of heat, moisture, and carbon fluxes *J. Hydrometeorol.* **15** 489–503

Krinner G *et al* 2005 A dynamic global vegetation model for studies of the coupled atmosphere–biosphere system *Glob. Biogeochem. Cycles* **19** GB1015

Li Z X 1999 Ensemble atmospheric GCM simulation of climate interannual variability from 1979 to 1994 *J. Clim.* **12** 986–1001

Mahowald N, Lo F, Zheng Y, Harrison L, Funk C and Lombardozzi D 2015 Leaf area index in Earth system models: evaluation and projections *Earth Syst. Dynam. Discuss.* **6** 761–818

Makarieva A M *et al* 2013 Where do winds come from? A new theory on how water vapor condensation influences atmospheric pressure and dynamics *Atmos. Chem. Phys.* **13** 1039–56

McMahon S M, Parker G G and Miller D R 2010 Evidence for a recent increase in forest growth *Proc. Natl Acad. Sci. USA* **107** 3611–5

Nemani R R *et al* 2003 Climate-driven increases in global terrestrial net primary production from 1982 to 1999 *Science* **300** 1560–3

Oleson K W *et al* 2010 *Technical Description of Version 4.0 of the Community Land Model (CLM)* (Boulder, CO: NCAR) (doi:10.5065/D6FB50WZ)

Pfeifer M *et al* 2014 Validating and linking the GIMMS leaf area index (LAI3g) with environmental controls in tropical Africa *Remote Sens.* **6** 1973–90
Piao S *et al* 2015 Detection and attribution of vegetation greening trend in China over the last 30 years *Glob. Change Biol.* **21** 1601–9
Sellers P J *et al* 1997 Modeling the exchanges of energy, water, and carbon between continents and the atmosphere *Science* **275** 502–9
Sewall J O, Sloan L C, Huber M and Wing S 2000 Climate sensitivity to changes in land surface characteristics *Glob. Planet. Change* **26** 445–65
Shao P *et al* 2013 Terrestrial carbon cycle: climate relations in eight CMIP5 Earth System Models *J. Clim.* **26** 8744–64
Shukla J and Mintz Y 1982 Influence of land-surface evapotranspiration on the Earth's climate *Science* **215** 1498–501
Sitch S *et al* 2015 Recent trends and drivers of regional sources and sinks of carbon dioxide *Biogeosciences* **12** 653–79
Stocker T F *et al* 2013 *Climate Change 2013 The Physical Science Basis: Contribution of Working Group I to The Fifth Assessment Report of the IPCC* (New York: Cambridge University Press) (doi:10.1017/CBO9781107415324)
Taylor K E, Stouffer R J and Meehl G A 2012 An overview of CMIP5 and the experiment design *Bull. Am. Meteorol. Soc.* **93** 485–98
Trenberth K E, Fasullo J T and Kiehl J 2009 Earth's global energy budget *Bull. Am. Meteorol. Soc.* **90** 311–23
Zeng N, Neelin J D, Lau K M and Tucker C J 1999 Enhancement of interdecadal climate variability in the Sahel by vegetation interaction *Science* **286** 1537–40
Zeng Z, Wang T, Zhou F, Ciais P, Mao J, Shi X and Piao S 2014 A worldwide analysis of spatiotemporal changes in water balance based evapotranspiration from 1982 to 2009 *J. Geophys. Res. Atmos.* **119** 1186–202
Zhang K *et al* 2015 Vegetation greening and climate change promote multidecadal rises of global land evapotranspiration *Sci. Rep.* **5** 15956
Zhang K, Kimball J S, Nemani R R and Running S W 2010 A continuous satellite-derived global record of land surface evapotranspiration from 1983 to 2006 *Water Resour. Res.* **46** W09522
Zhang Y *et al* 2016 Multi-decadal trends in global terrestrial evapotranspiration and its components *Sci. Rep.* **6** 19124
Zhu Z *et al* 2013 Global data sets of vegetation leaf area index (LAI) 3 g and fraction of photosynthetically active radiation (FPAR) 3 g derived from Global Inventory Modeling and Mapping Studies (GIMMS) Normalized Difference Vegetation Index (NDVI3g) for the period 1981 to 2011 *Remote Sens.* **5** 927–48
Zhu Z *et al* 2016 Greening of the Earth and its drivers *Nat. Clim. Change* **6** 791–5